Supplementary Information

for

Depth Mapping of Metallic Nanowire Polymer Nanocomposites by Scanning Dielectric Microscopy

Harishankar Balakrishnan[1§], Ruben Millan-Solsona[1§], Marti Checa[1], Rene Fabregas[2], Laura Fumagalli[2,3] and Gabriel Gomila[*,1,4]

[1]*Institut de Bioenginyeria de Catalunya (IBEC), The Barcelona Institute of Science and Technology (BIST), c/ Baldiri i Reixac 11-15, 08028, Barcelona, Spain*

[2]*Department of Physics and Astronomy, University of Manchester, Manchester M13 9PL, UK*

[3]*National Graphene Institute, University of Manchester, Manchester M13 9PL, UK4*

[4]*Departament d'Enginyeria Electrònica i Biomèdica, Universitat de Barcelona, C/ Martí i Franqués 1, 08028, Barcelona, Spain*

[§]Equally contributing Authors. *Corresponding author: ggomila@ibecbarcelona.eu

S1. Additional data Fig. 2: photodiode and tip geometry calibration and gelatin dielectric constant determination.

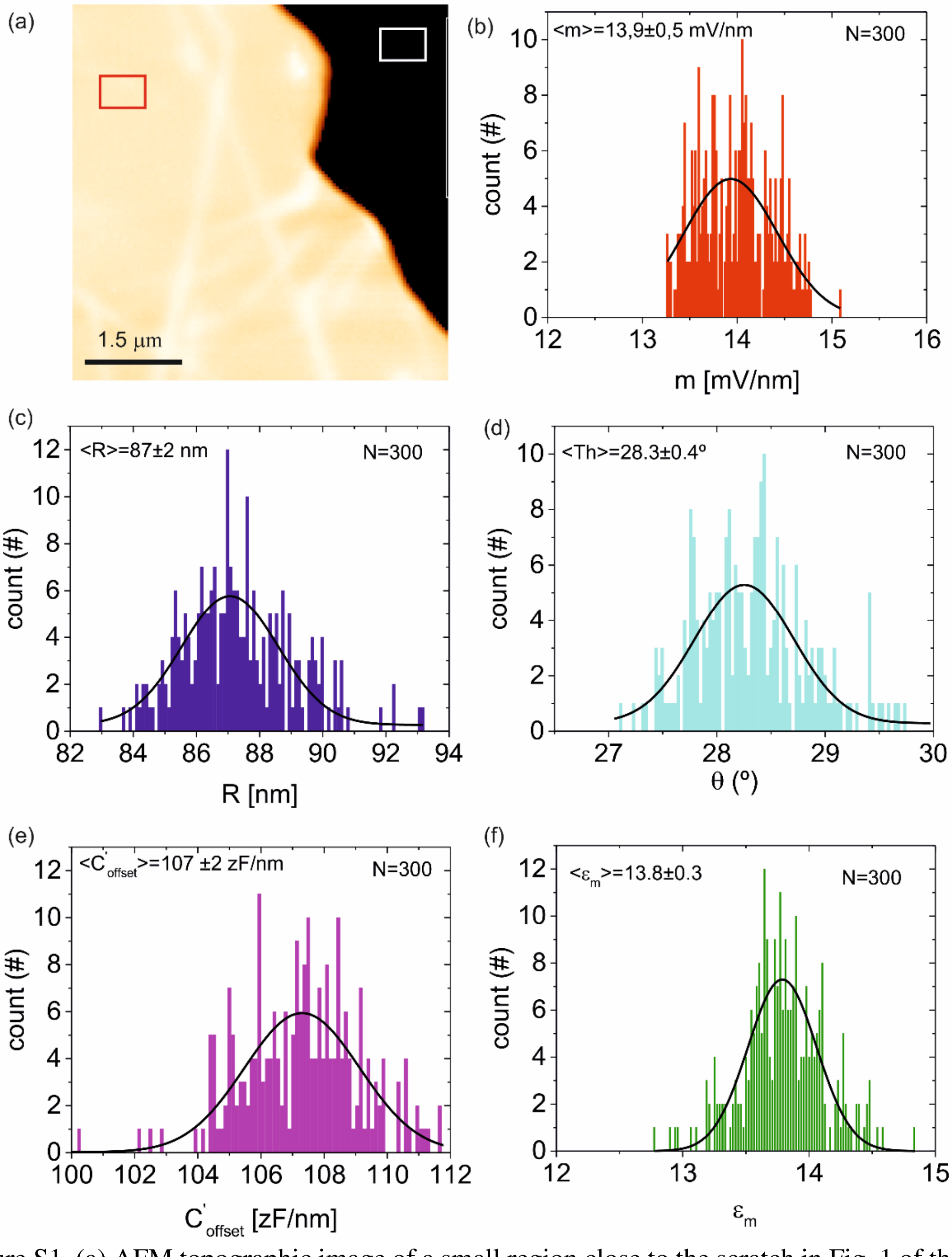

Figure S1. (a) AFM topographic image of a small region close to the scratch in Fig. 1 of the main text. The white and red rectangles highlight the regions used to calibrate the photodiode sensitivity and tip geometry and to extract the dielectric constant of gelatin, respectively. (b) Distribution of the photodiode sensitivity extracted from the slope of the contact part of the normal deflection approach curves. The mean value (N=300) is 13.9±0.5 mV/nm. (c)-(e) Histogram of the tip radius, half cone angle and capacitance gradient offset obtained by fitting theoretical dC/dz curves generated for a tip-on-metal model to the experimental dC/dz approach curves acquired in the white rectangle region in (a). The mean values (N=300) obtained are R=87±2 nm, θ=28.3±0.4º and C'_{offset}=107±2 zF/nm, respectively. (f) Histogram distribution of the values obtained for the dielectric constant of gelatin obtained by fitting theoretical dC/dz curves generated for a tip-on-thin dielectric film model to the experimental dC/dz approach curves acquired in red rectangle in (a). The mean value (N=300) obtained is ε_m=13.8±0.3.

S2. Effect of the nanowire diameter in the estimation of the depths.

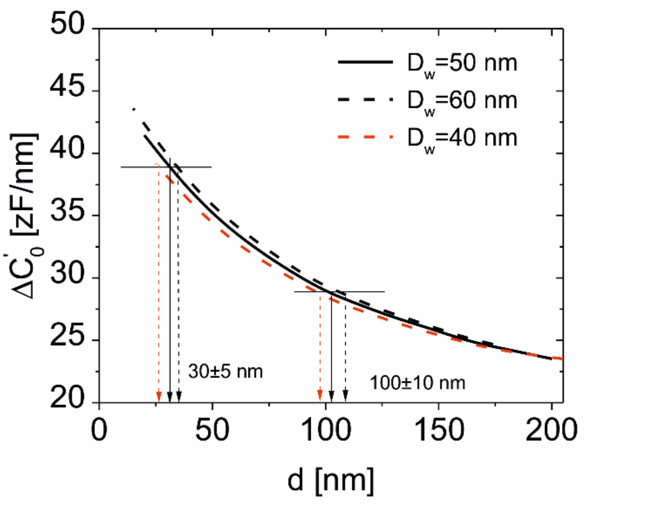

Figure S2. Capacitance gradient contrast at the center of a buried nanowire, $\Delta C'_0$, calculated with the model in Fig. 2k of the main text as a function of the depth, for three nanowire diameters D_w=40 nm, 50 nm and 60 nm and a surface protrusion h_p=8 nm. The tip is located at a height z=36 nm from the flat surface. From this graph we can estimate that a variation of ±10 nm of the nanowire diameter of 50 nm induces at most an error of ±5 nm in the estimation of the depth. Parameters: same as those in Fig. 2.

S3. Effect of the length of the nanowire in the estimation of the depth

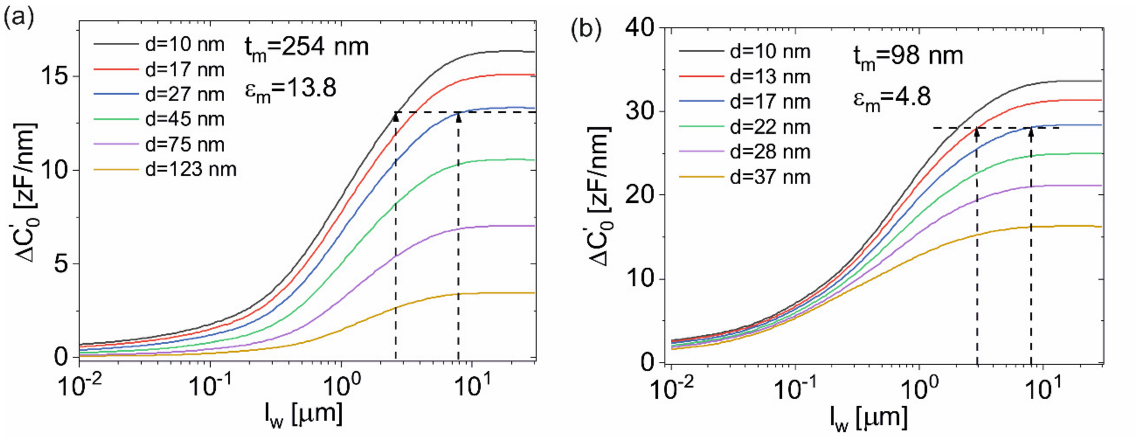

Figure S3. (a) Capacitance gradient contrast at the center of a buried nanowire for the tip at a distance z=36 nm from the surface of the gelatin film as a function of the length of the nanowire, for different depths, d, with no surface h_p=0 nm. Parameters of the calculations: Same as for Fig. 2 of the main text. For lengths larger than l_w~8 μm (the one used in the main text) the results become independent from the length. If a nanowire is shorter, one can estimate the depth as indicated by the arrows in the graph. (b) Idem for the case of parameters corresponding to Fig. 4 of the main text.

S4. Inclined vs non-inclined nanowire models

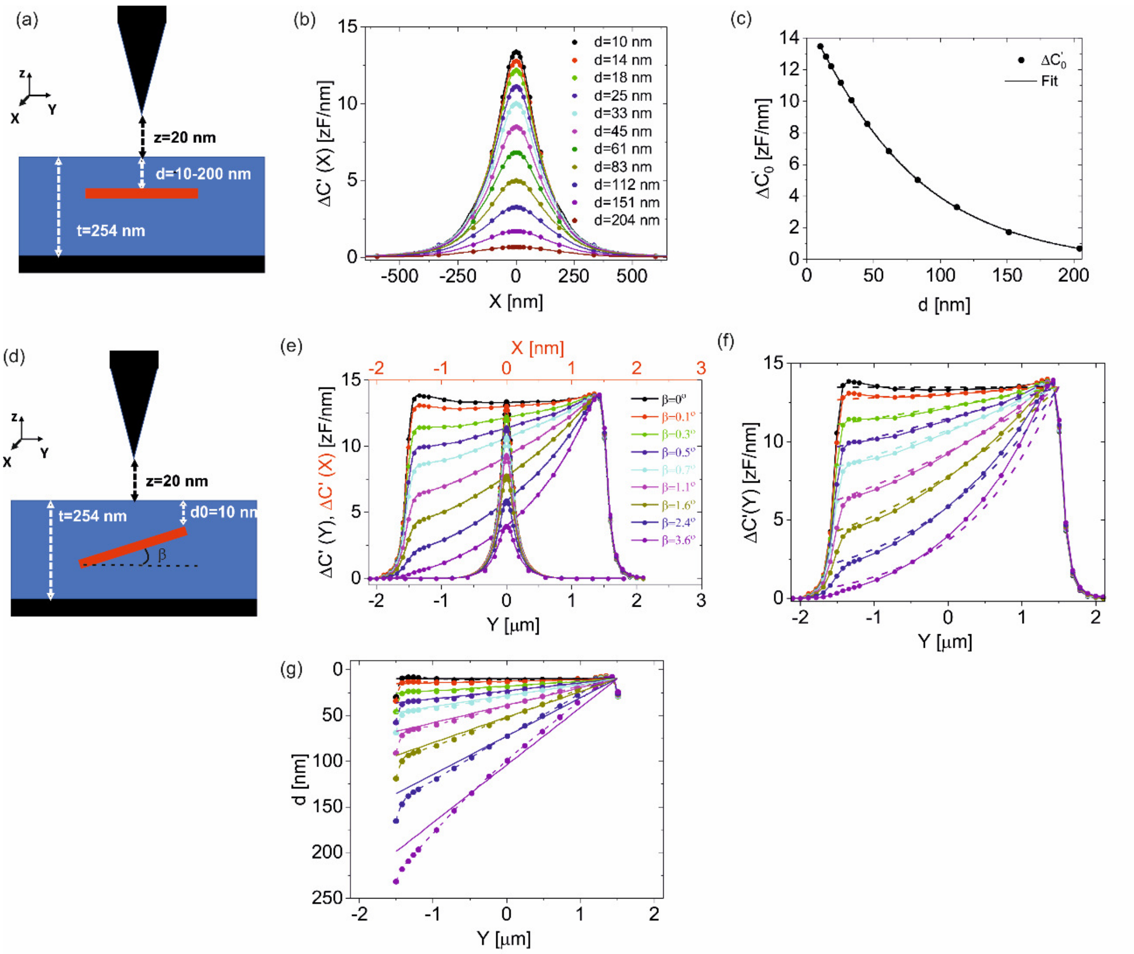

Figure S4. (a) Schematic representation of a model of a buried nanowire parallel to the substrate (same model as the one used in the main text, without the surface protrusion). (b) Cross-section capacitance gradient contrast profiles along the transversal direction to the nanowire, ΔC'(X), for different depths, d. (c) (symbols) Capacitance gradient contrast at the center of the wire, $\Delta C'_0$, as a function of the depth. (continuous line) Least square fitting of the function $\Delta C_0^{'}(d) = A(1+Bd)/(1+Cd+Dd^2)$, with A=15.1 zF/nm, B=-3.7·10^{-3}nm^{-1}, C=7.1·10^{-3}nm^{-1}, D=7.0·10^{-5}nm^{-2}. (d) Schematic representation of a model of a buried nanowire inclined an angle β with respect to the substrate. (e) Capacitance gradient contrast profiles along the transversal, ΔC'(X), (black symbols, left and bottom axes) and longitudinal, ΔC'(Y), (red symbols, right and top axis) directions, respectively. (f) (dashed lines) Capacitance gradient contrast profile along the nanowire, ΔC'(Y), calculated by using the function $\Delta C_0^{'}(d)$ in (c) and the depth profile of an inclined nanowire, $d(Y) = d_0 + \left[(l_w/2)\cos(\beta) - Y\right]\tan(\beta)$. The symbols and continuous lines correspond to the numerically calculated profiles (same as in (e)). (g) (symbols with dashed lines) Local nanowire depths extracted with the function $\Delta C_0^{'}(d)$ applied to the profiles of the inclined nanowires in (e), ΔC'(Y). The extracted depths nicely reproduce the actual nanowire depth profiles (continuous lines). This result demonstrates that the non-inclined nanowire model can be used to predict the local depth of inclined nanowires, as we did in the manuscript. Parameters used in the calculations: D_w=50 nm, l_w=3 µm, ε_w=10^5 (metallic), d_0=10 nm, t_m=254 nm, ε_m=13.8, R=87 nm, θ=28°, H=12.5 µm, W=3 µm, L=3 µm.

S5. Additional data Fig. 4: photodiode and tip geometry calibration, and gelatin dielectric constant determination.

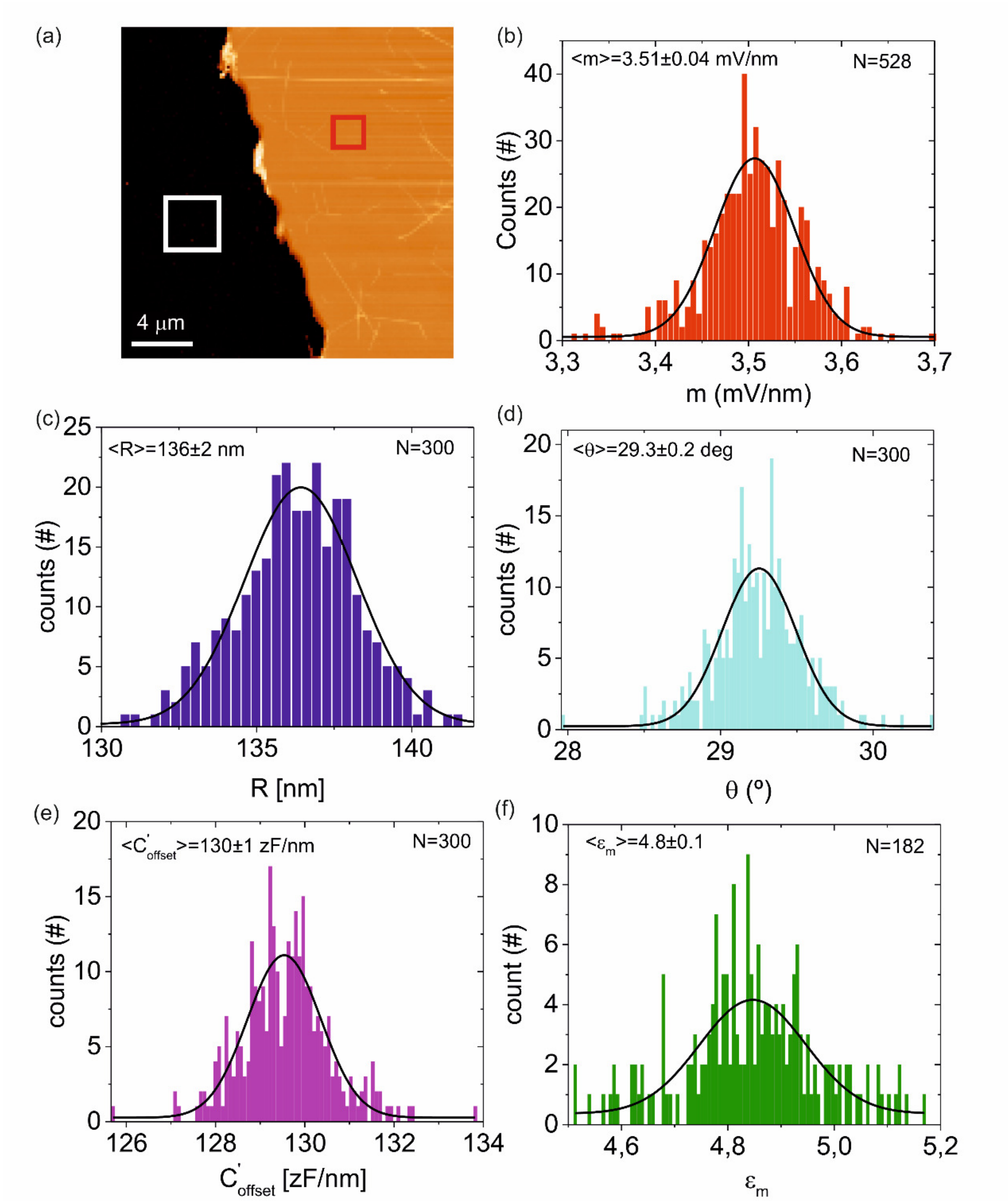

Figure S5. (a) AFM topographic image of a larger region corresponding to Fig. 4 of the main text. The white and red rectangles highlight the regions used to calibrate the photodiode sensitivity and tip geometry and to extract the dielectric constant of gelatin, respectively. (b) Distribution of the photodiode sensitivity extracted from the slope of the contact part of the normal deflection approach curves. The mean value (N=528) is 3.51±0.04 mV/nm. (c)-(e) Histogram of the tip radius, half cone angle and capacitance gradient offset obtained by fitting theoretical dC/dz curves generated for a tip-on-metal model to the experimental dC/dz approach curves acquired in the white rectangle region in (a). The mean values (N=300) obtained are R=136±2 nm, θ=29.3±0.2º and C'_{offset}=130±1 zF/nm, respectively. (f) Histogram distribution of the values obtained for the dielectric constant of gelatin obtained by fitting theoretical dC/dz curves generated for a tip-on-thin dielectric film model to the experimental dC/dz approach curves acquired in red rectangle in (a). The mean value (N=300) obtained is ε_m=4.8±0.1

S6. Examples of experimental capacitance gradient approach curves and of the corresponding fitted curves.

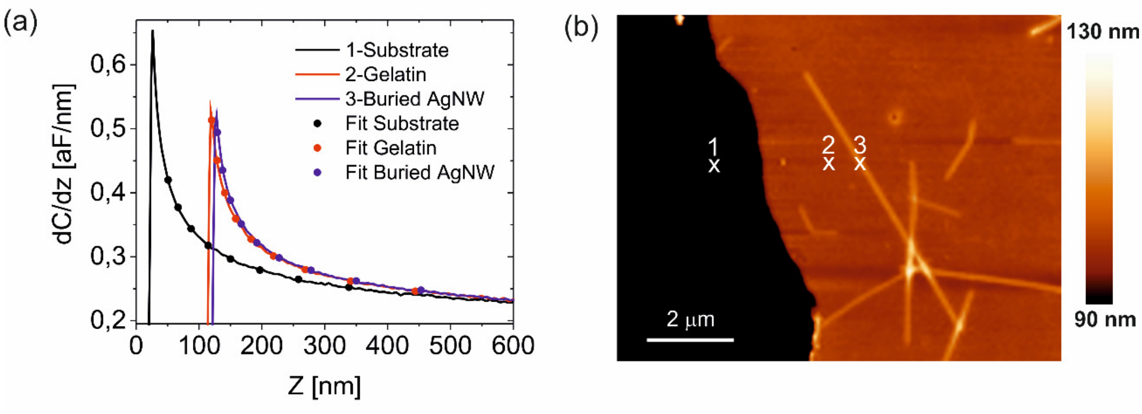

Figure S6. (a) (continuous lines) Examples of experimental capacitance gradient approach curves, dC/dz, corresponding to three pixels of the image in Fig. 4 of the main manuscript at the positions indicated by the crosses in (b). The symbols represent the corresponding least square fitted theoretical curves. The theoretical curve on the substrate is generated from a tip-flat metal model, that on the gelatin from a tip-thin film dielectric model and that on the buried nanowire from the model in Fig. 2k of the main manuscript. From the fit on the substrate curve one obtains the tip geometry, from that on the gelatin the dielectric constant of gelatin and from that on the buried nanowire the depth position.